Ambient and forced-vibration tests of the Beauharnois suspension bridge

P. Paultre, J. Proulx, and T. Bégin

Abstract: Ambient and forced vibration tests were carried out on the Beauharnois Bridge, a unique, 177-m combined suspension and cable-stayed structure near Montreal. A rehabilitation program was completed on the bridge during which the deck was completely rebuilt with an orthotropic slab on two steel trusses. The rehabilitation program also included the addition of two pairs of stay cables on both towers, creating a hybrid suspension system. The paper presents a series of dynamic tests performed to evaluate the dynamic properties and the dynamic amplification factor (DAF) for the rehabilitated bridge. The experimental program involved the measurement of vertical, transverse, and longitudinal acceleration responses of the deck and tower under ambient and controlled traffic loads. Displacement, strain, and integrated acceleration DAFs were computed under different loading conditions. Modal properties were evaluated and used to correlate a three-dimensional finite element model for the bridge, including nonlinear cable behaviour. The paper discusses the experimental setup and the techniques used to evaluate vibration frequencies, mode shapes, and the DAF. Correlation of numerical dynamic properties and experimental results is also presented.

Key words: cable-stayed bridge, dynamic amplification, dynamic testing, numerical correlation, modal analysis, suspension bridge.

Résumé: Des essais de vibrations ambiantes et forcées ont été effectués sur le pont de Beauharnois, une structure unique de 177-m à suspension et à haubans combinés, près de Montréal. Un programme de réhabilitation a été réalisé sur le pont pendant lequel le tablier a été complètement reconstruit avec une dalle orthotropique sur deux fermes en acier. Le programme de réhabilitation a également inclus l'ajout de deux paires de haubans sur les deux tours, créant un système de suspension hybride. L'article présente une série d'essais dynamiques réalisés pour évaluer les propriétés dynamiques et le facteur d'amplification dynamique (FAD) pour le pont remis en état. Le programme expérimental a comporté la mesure des réponses verticales, transversales, et longitudinales d'accélération du tablier et de la tour sous des charges ambiantes et contrôlées de la circulation. Les FAD sur déplacement, la déformation, et l'accélération intégrée ont été calculés sous différentes conditions de charge. Les propriétés modales ont été évaluées et employées pour corréler un modèle tridimensionnel d'éléments finis pour le pont, comprenant le comportement non linéaire des câbles. L'article discute l'installation expérimentale ainsi que les techniques employées pour évaluer les fréquences de vibration, les formes des modes, et le FAD. La corrélation entre les propriétés dynamiques numériques et les résultats expérimentaux est également présenté.

Mots clés: pont haubanné, amplification dynamique, essai dynamique, corrélation numérique, analyse modale, pont suspendu.

[Traduit par la Rédaction]

1. Introduction

The dynamic behaviour of long-span suspension and cable-stayed bridges is usually the predominant parameter in the determination of project feasability. In particular, sufficient separation of flexural and torsional modes is important to avoid aerodynamic problems. Wind tunnel tests are usually carried out on complete or partial bridge models. In both cases, accurate knowledge of the dynamic properties is required for such studies. The most reliable means of verifying the predictions of these properties is to conduct full-scale dynamic tests on the completed structure.

With the availability of affordable and reliable testing equipment, there has been a considerable increase in large-scale structural testing. This can be observed by the growing number of published papers and reports on the experimental study of bridge dynamics (Paultre et al. 1992; Murià-Villa et al. 1991; Stiemer et al. 1988; Wilson and Gravelle 1991; Wilson and Liu 1991). Most dynamic tests today are carried out to evaluate dynamic properties for the calibration of finite element models or to monitor changes in a specific bridge's dynamic behaviour. In the past, a large number of dynamic tests of short- and medium-span bridges have also been performed to determine the dynamic amplification factor (DAF) generated by ambient or controlled traffic loads. However, this parameter is rarely measured for long-span cable-supported bridges. Indications about the dynamic amplification or impact factor are needed for these types of bridges, as values found in design codes are usually limited to bridges with span lengths under 100 m.

This paper presents the experimental procedures used for testing the Beauharnois Bridge, which has the unusual feature

Received July 16, 1999.
Revised manuscript accepted May 10, 2000.

P. Paultre[1] **and J. Proulx.** Department of Civil Engineering, Faculty of Engineering, Université de Sherbrooke, 2500, boul. de l'université, Sherbrooke, QC J1K 2R1, Canada.
T. Bégin. Steel-Plus Network (Canam), 11535, 1ére ave., bureau 500, St-Georges, QC G5Y 7H5, Canada.

Written discussion of this article is welcomed and will be received by the Editor until April 30, 2001.

[1]Author to whom all correspondence should be addressed (e-mail: ppaultre@gci.usherb.ca).

Fig. 1. Beauharnois suspension bridge: (*a*) plan view and (*b*) elevation view.

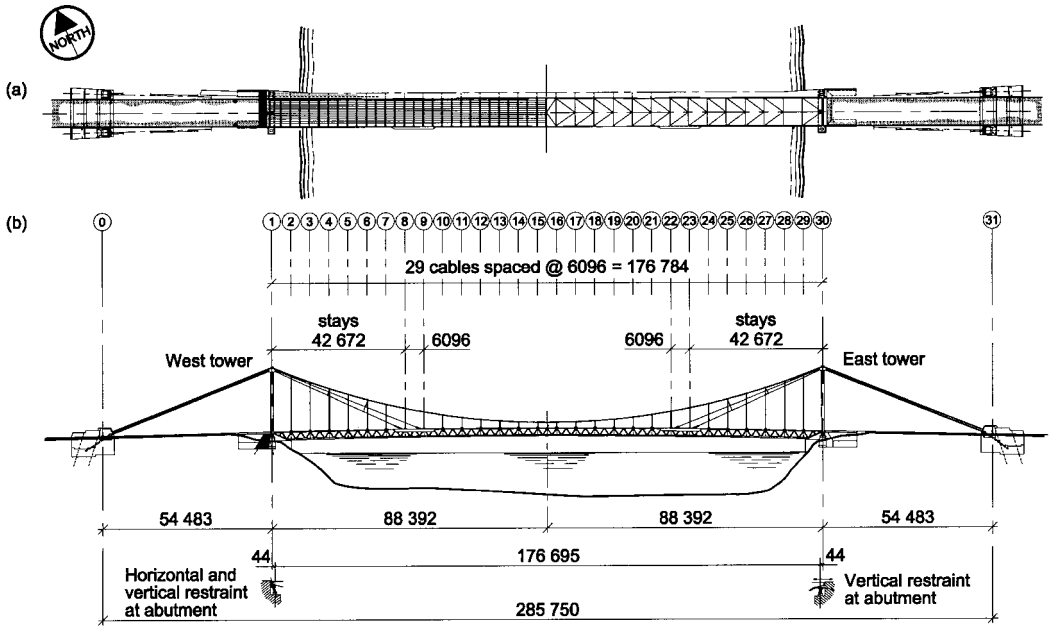

Fig. 2. Beauharnois suspension bridge: (*a*) tower elevation, (*b*) cross section at midspan, and (*c*) cross section at support.

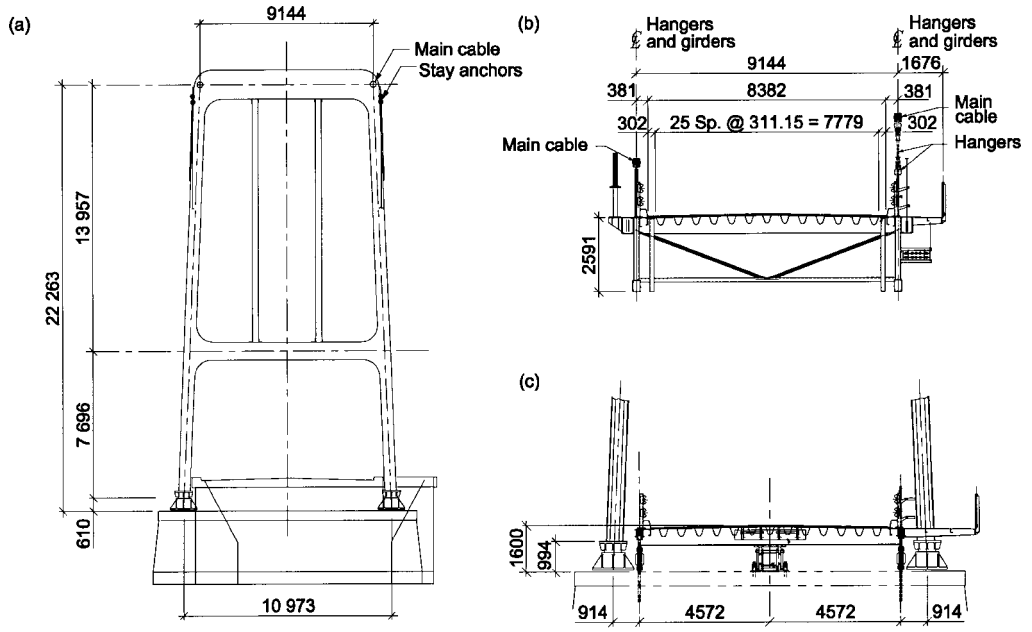

of having a hybrid suspension and cable-stayed main structural system. The determination of the dynamic properties and dynamic amplification factors is discussed, with emphasis on the instrumentation, data processing, and numerical correlation with a finite element model including nonlinear cable behaviour.

2. Beauharnois Bridge

The Beauharnois suspension bridge crosses the Saint Lawrence River 40 km southeast of Montreal. It has two traffic lanes, a 177-m span, and two 22.26-m towers. Built in 1947, the bridge consisted of two stiffening built-up steel girders supporting crossbeams and stringers. Longitudinal forces from the main girders were transferred to the suspension cables at their lowest points by means of two sets of inclined hangers. The original concrete bridge deck has deteriorated throughout the years under increasing truck loads and repeated application of de-icing salt during the winter. In 1987, the speed limit had to be reduced and traffic restricted to only one lane in order to maintain an acceptable level of safety.

In 1988, the owner opted to rehabilitate the damaged bridge. Economical considerations led to a rehabilitation program that maintained the main cables and the towers. The major por-

Fig. 3. Instrumentation setup: (*a*) plan view and (*b*) elevation view for positions of accelerometers and (*c*) position of strain gauges.

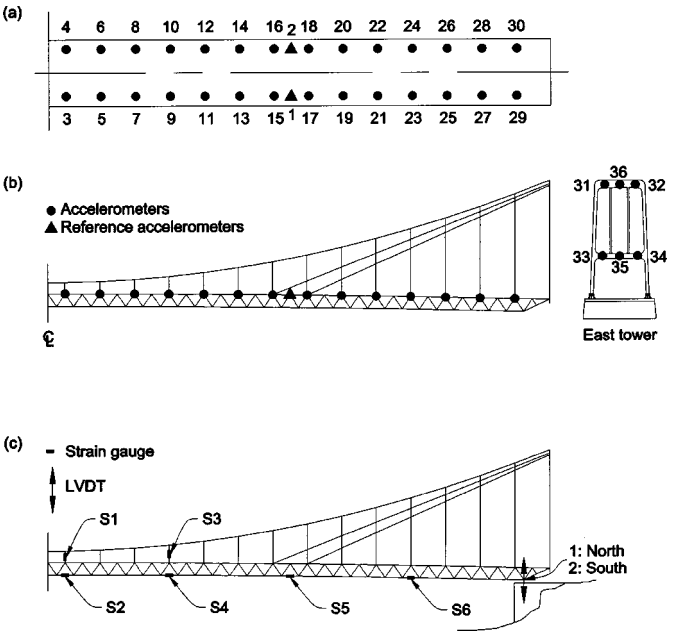

tions of the work included (*i*) a complete replacement of the roadway by an orthotropic deck supported by two transversally braced stiffening hollow-tube steel trusses; (*ii*) the addition of two pairs of stay cables on each tower in order to keep the existing suspension cables and increase overall bridge capacity; and (*iii*) the horizontal anchoring of the deck on one of the abutments to transfer longitudinal forces directly to the foundation and reduce cable loads. These modifications were completed in 1989 and the new bridge, which now has a hybrid suspended and cable-stayed behaviour, is presented in Figs. 1 and 2. Aerodynamic studies were conducted on a partial model of the new structure using analytical predictions of the dynamic properties.

3. Instrumentation

The experimental evaluation of the modal properties of the Beauharnois Bridge was carried out by frequency analysis of acceleration data obtained under normal traffic loads, without blocking access to the structure. It was also possible to periodically restrict the access to the bridge and, therefore, to use controlled traffic loading with test vehicles crossing the bridge at different speeds and positions.

One of the objectives of the dynamic tests carried out on the Beauharnois Bridge was to determine modal properties. In addition, in the design phase of the rehabilitation work, it became apparent that reliable data were lacking on the dynamic amplification factor (DAF) applicable to long-span (over 100 m) suspension bridges. This factor is the ratio of the maximum dynamic response of the bridge to the maximum static response under traffic loads. Its purpose is to amplify the static forces and displacements in the design or rehabilitation process, as specified by bridge design codes, to take into account the effects of bridge–vehicle interaction. Therefore, the tests were also designed to obtain the structure's average DAF, which must be

Fig. 4. Test vehicles and loads: (*a*) 10-wheel truck and (*b*) trailer.

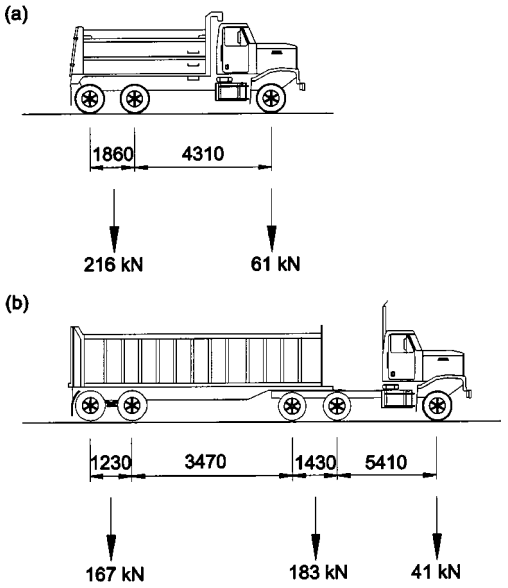

evaluated using test vehicles of known weight, hence the need for controlled traffic tests.

The series of dynamic tests on the the Beauharnois Bridge were part of a larger research program sponsored by the Quebec Ministry of Transportation (MTQ) on the dynamic behaviour of highway bridges and the experimental evaluation of the dynamic amplification factor. Large-scale dynamic testing procedures that were developed and applied on a series of bridges are summarized below; more details can be found in Paultre et al. (1995).

The experimental setup used on the Beauharnois Bridge is shown in Fig. 3. Instrument locations were chosen to obtain a maximum number of flexural and torsional modes. Half of the symmetric deck was instrumented at each vertical hanger attachment point. Vertical, transverse, and longitudinal accelerations were obtained with eight low-frequency, force-balanced accelerometers. These instruments have a 50-Hz cutoff frequency with a flat response up to 10 Hz. This range is sufficient to identify a large number of modes for most suspended bridges, which are usually characterized by very low frequencies for their fundamental resonances. Three pairs of accelerometers were successively placed at each of the 14 positions on both sides of the deck. Two accelerometers remained at reference stations 1 and 2 throughout the tests, which are located halfway between the stay-cable anchor points on both sides of the deck (Fig. 3*a*). Only three accelerometer configurations were necessary to cover all measurement stations on the deck. Accelerometers were also placed inside the east tower to record longitudinal and transverse motions.

To measure bridge vertical displacement, two linear variable differential transducers (LVDTs) were placed underneath the lower chord of the main truss at the east end of the bridge, close to accelerometer positions 29 and 30, as shown in Fig. 3*c*. Due to the heavy current of the river, LVDTs could not be placed elsewhere. However, as will be dicussed below, displacements were also obtained by integration of acceleration recordings.

Strain measurements were obtained on two vertical hangers (positions S1 and S3 in Fig. 3*c*). All vertical hangers are made

Fig. 5. View of test vehicle on bridge.

Table 1. Dynamic tests on the Beauharnois Bridge.

Type of test	Instrument positions	Vehicle(s)	Number of runs	Direction of recording
Normal traffic	Deck	—	34	Vertical
	Deck	—	15	Longitudinal
	Deck	—	15	Transverse
	Tower	—	6	Longitudinal and transverse
Controlled traffic	Deck	Single truck	16	Vertical
	Deck	Single truck	7	Longitudinal
	Deck	Single truck	2	Transverse
	Tower	Single truck	3	Longitudinal and transverse
	Deck	Truck and trailer	16	Vertical
	Deck	Truck and trailer	7	Longitudinal
	Deck	Truck and trailer	2	Transverse
	Tower	Truck and trailer	3	Longitudinal and transverse
	Deck	Two trucks side-by-side	6	Vertical
	Deck	Two trucks in line	12	Vertical
Total			144	

of 30-mm steel cable, with the exception of hangers 12 to 19 (Fig. 1), which are made of two steel plates. Strain gauges were glued directly on hangers 16 and 19. The lower chord of the main truss was also instrumented with strain gauges at hangers 12, 19, and 26 and at the location of the reference accelerometers (positions S2, S4, S5, and S6 in Fig. 3*c*). The recorded displacements and strains were used to evaluate the maximum dynamic and static responses of the structure under controlled traffic and subsequently the DAF.

Each instrument was connected to an HP3852a data-acquisition system with track-and-hold capabilities and a 100 000-Hz aggregate sampling rate. Data were typically sampled at 100 Hz for 120 s. Hardware filters with 20-Hz cutoff frequency were used to eliminate aliased frequencies. The acquisition process is entirely computer-controlled with software developed at the Université de Sherbrooke. The use of customized software is often the only way to have control over crucial parameters like sampling frequency, total sampling time, and filtering, since most commercial packages are not implemented specifically for large civil-engineering structures. The evaluation of frequencies, mode shapes, and modal damping for such structures often requires a resolution below 0.05 Hz in the frequency domain.

4. Testing procedure

As mentioned above, two different series of dynamic tests were carried out on the bridge. In the first series, acceleration data were measured under normal traffic (ambient) conditions. The second series of tests was conducted with controlled traffic to obtain the dynamic amplification factor.

Fig. 6. Example of measured responses for a controlled traffic run, single truck (center) at 76 km/h: (*a*) vertical reference accelerometer, (*b*) accelerometer on deck at station 7, (*c*) displacement transducer 1, (*d*) strain gauge 2, and (*e*) pressure tube.

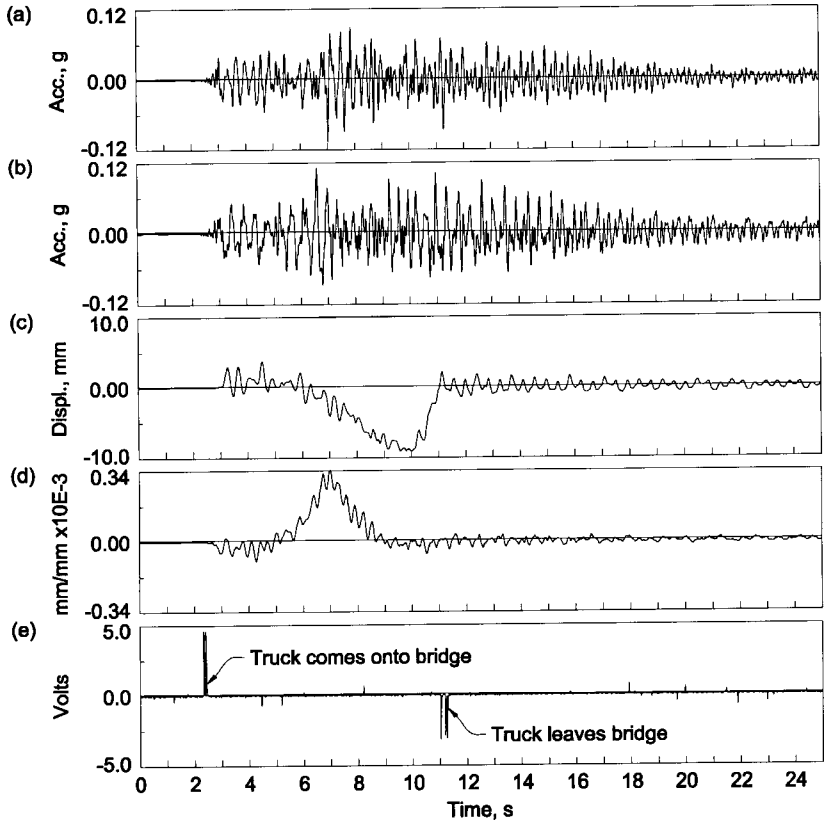

The ambient vibration tests included a total of 70 recordings obtained by successively moving the accelerometers at every station on the deck and the east tower. For each position, measurements were taken in the longitudinal, transverse, and vertical directions. Six 120-s recordings were made for each instrument configuration. It was determined on site from frequency analysis of the recorded data (see below) that taking the average of at least three recordings was necessary for the stability of the frequency response curves. Moreover, the computed curves did not vary when using more than six recordings for a given configuration.

The second series of tests was carried out with selected vehicles to evaluate the DAF. Two 277-kN, 10-wheel trucks and a 391-kN trailer were provided by the MTQ for the tests (Fig. 4). With traffic blocked periodically, the test vehicles completed a total of 74 runs at different speeds and positions on the bridge. Vehicle speeds, which varied from 13 to 82 km/h, were recorded with a traffic counter that emitted a pulse when the vehicles came onto or left the bridge. Figure 5 shows a 391-kN trailer in the right lane. Side-by-side and in-line configurations were also used. Table 1 lists the type and number of tests as well as the instrument configurations used during the tests.

Figure 6 illustrates time history plots of recorded data for a single truck driving in the center of the roadway at an average speed of 76 km/h (the speed limit is 90 km/h). The pulse signals generated by pressure tubes placed at both ends of the span are shown in the bottom graph in Fig. 6*e*. Different peaks on the graph correspond to different axles entering or leaving the bridge. A peak-detection program is used to determine the time values at which the pulses occur; the average speed of the vehicle is then computed for each run. Figure 6*a* represents the acceleration time history obtained at the reference station in the vertical direction. The next graph (Fig. 6*b*) shows the vertical acceleration response recorded at station 7 on the deck. The displacement response obtained for the displacement transducer (LVDT) at position 1 is shown in Fig. 6*c*, and Fig. 6*d* illustrates the strain measurements obtained at station S2 on the lower chord of the main truss. These two influence lines clearly show the dynamic component superposed on the static response.

The peak accelerations were recorded on the deck in the vertical direction for both ambient and controlled traffic tests (see Table 2). The table shows that these values were obtained at the maximum speeds and that a single truck or two trucks in both configurations produced twice the acceleration obtained by the truck and trailer.

5. Dynamic properties

One of the primary objectives of the Beauharnois Bridge tests was to evaluate the DAF; this required that the structure be tested under controlled traffic loads. With this type of excitation the input forces, which are needed for true modal analysis techniques, are not usually measured. The frequencies and mode shapes are then evaluated by a derived technique in which a recorded response is used as a system "input", called a reference signal. Recordings from all other measurement stations are considered responses to this input.

Fig. 7. Frequency contents of normal traffic acceleration responses.

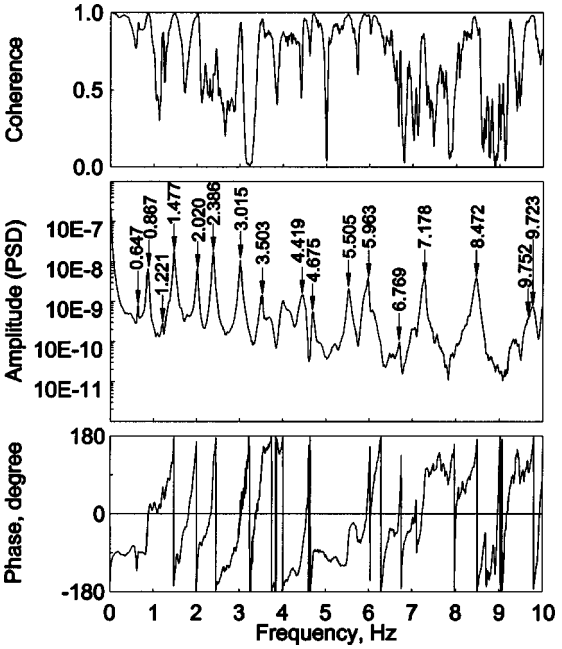

Table 2. Peak vertical accelerations recorded on the deck.

Type of test	Speed (km/h)	Peak acceleration (*g*)
Normal traffic	—	0.112
Single truck	75	0.189
Truck and trailer	80	0.108
Two trucks in line	75	0.192
Two trucks side-by-side	75	0.203

Frequency contents are obtained for all recordings by Fast Fourier Transform (FFT). Cross spectra and coherence functions can then be evaluated and averaged for each measurement position with respect to the reference station (Paultre et al. 1995). Resonant frequencies are directly obtained from peaks in the amplitude of the FFT curves for each signal, ruling out peaks with low coherence values (typically below 0.8) associated with local modes or bridge–vehicle interaction. The FFTs are computed with an exponential window to reduce noise in the amplitude and phase, often present in the lower frequency values. A direction of motion is established with respect to the reference station using the phase values for each resonant frequency. The experimental mode shapes are then plotted for the instrumented part of the deck.

Suspension and cable-stayed bridges generally exhibit coupled torsional and flexural modes, which are closely spaced in the frequency domain and can be difficult to separate by inspecting the FFT curves (Fig. 7). This problem can often be solved by a technique that consists of adding or subtracting time-domain acceleration data obtained at the same positions but on both sides of the bridge deck. Adding the pair of signals emphasizes flexural modes, while subtracting data will isolate torsional modes. This is demonstrated in Fig. 8 which

Fig. 8. Frequency contents of normal traffic acceleration responses: (*a*) addition of vertical accelerations and (*b*) subtraction of vertical accelerations.

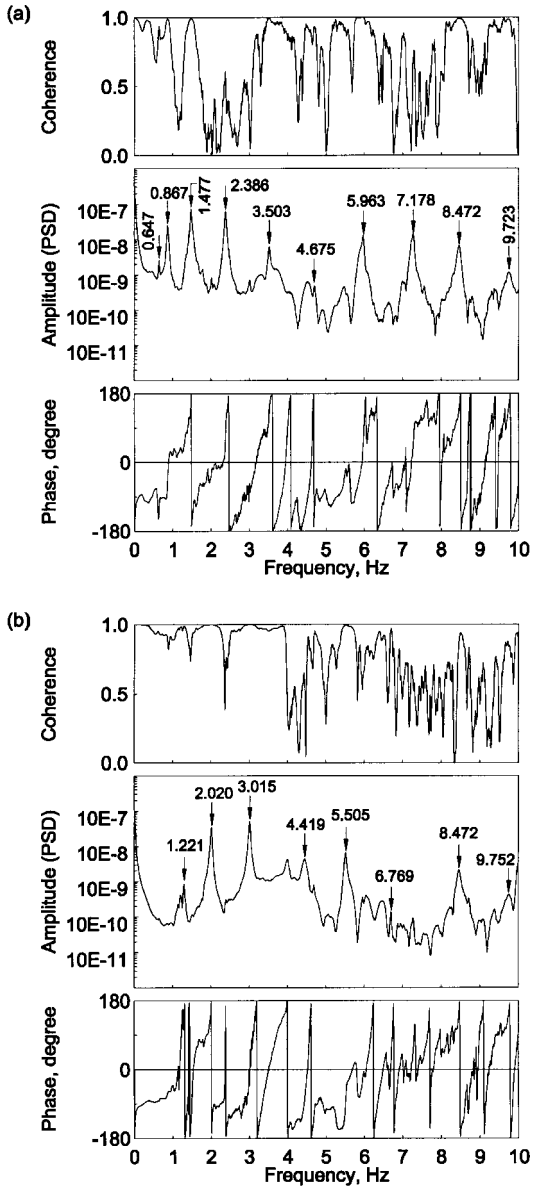

Fig. 9. Partial view of 3D finite element model of the bridge.

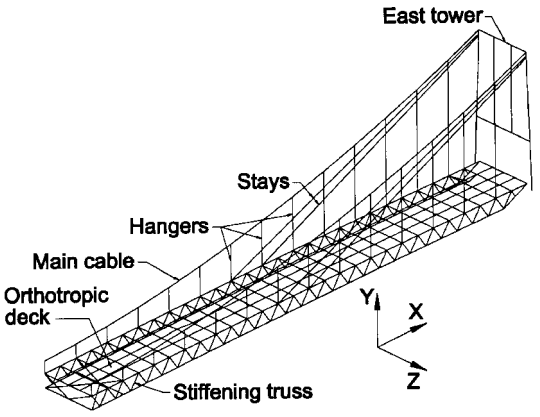

Fig. 10. Finite element model (fem) and experimental (exp) first flexural and torsional modes.

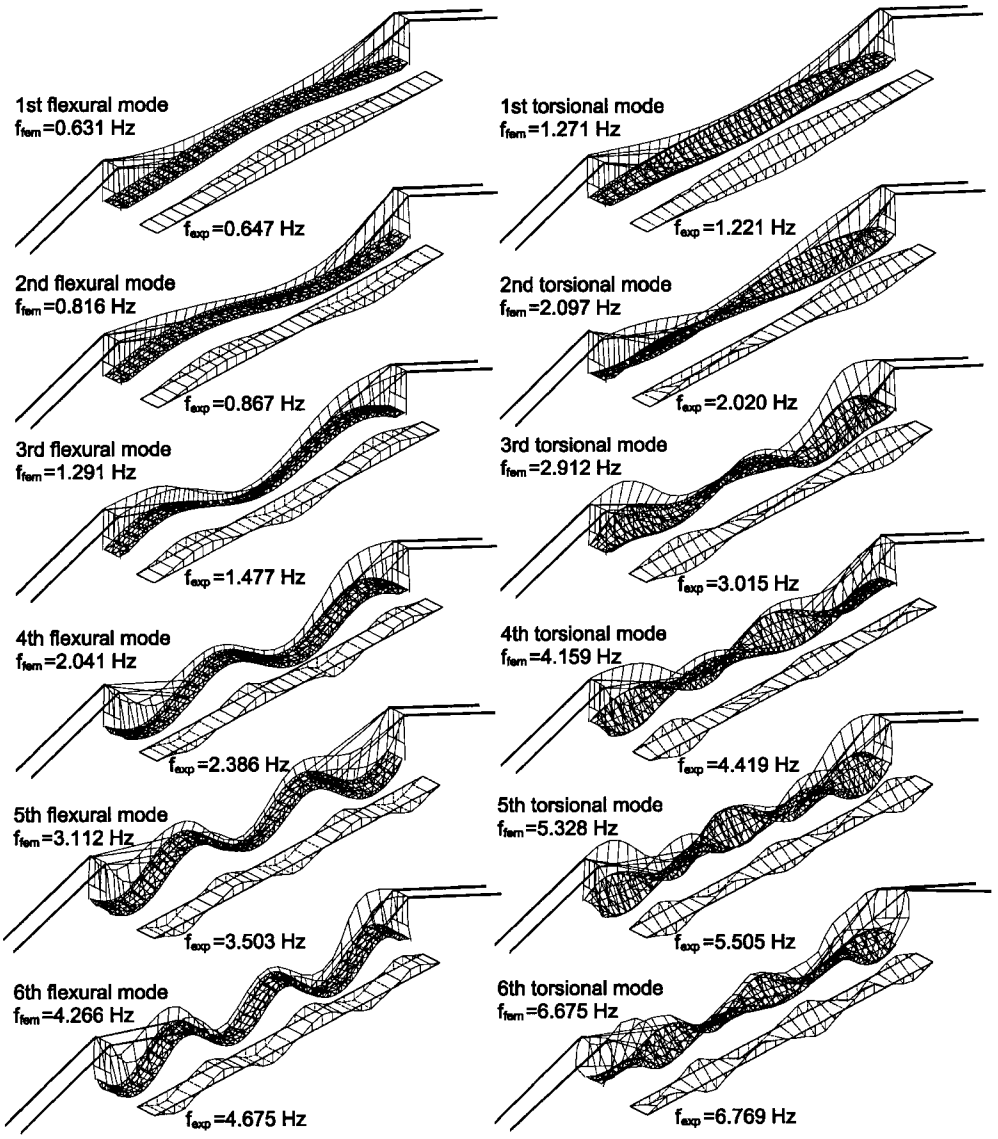

shows the amplitude of the FFTs obtained for a fixed position on the bridge from added and subtracted vertical acceleration responses. Flexural modes are identified with the added responses shown in Fig. 8*a*; torsional modes are taken from subtracted responses in Fig. 8*b*. The first six flexural and torsional modes obtained with this technique are shown in Fig. 10. Mode shapes for the towers were also obtained with a similar procedure, and the first six are illustrated in Fig. 11.

6. Numerical correlation

A three-dimensional finite element model was developed for the bridge and consists of 1377 nodes for a total of 2703 degrees of freedom (DOF). The actual geometry of the stiffening girder, main suspension cables, and stays were determined by following the sequence of construction. A partial view of half of the model is shown in Fig. 9.

In the first step, the stiffening girders were modeled by sections as-built to evaluate the tension in the main cables at the connection stage of the individual sections of the main girders and to evaluate the final position of the towers and the deck as well as the final geometry of the main cables. This computed geometry was then checked and adjusted with as-built geometry. Tension forces applied on the stay cables were used directly in the analysis.

All cables were modeled with elements that possess axial stiffness only under tensile load and whose transverse stiffness depends on cable axial tension. The main suspension cables were modeled with 30 linear cable elements with nodes at each junction with the vertical hangers, the towers, and anchorage points. This model allowed for the calculation of the global dynamic properties of the main cables. The hangers were each modeled with a single linear cable element with nodes attached to the main cables and the stiffening girders. The stay cables were modeled with single linear cable elements joining the towers to the stiffening girders. The use of single elements does not permit the evaluation of local hangers and stay modes, which were not part of the experimental program.

Fig. 11. Finite element model (fem) and experimental (exp) tower modes: (*a*) transverse modes, (*b*) longitudinal modes, and (*c*) torsional modes.

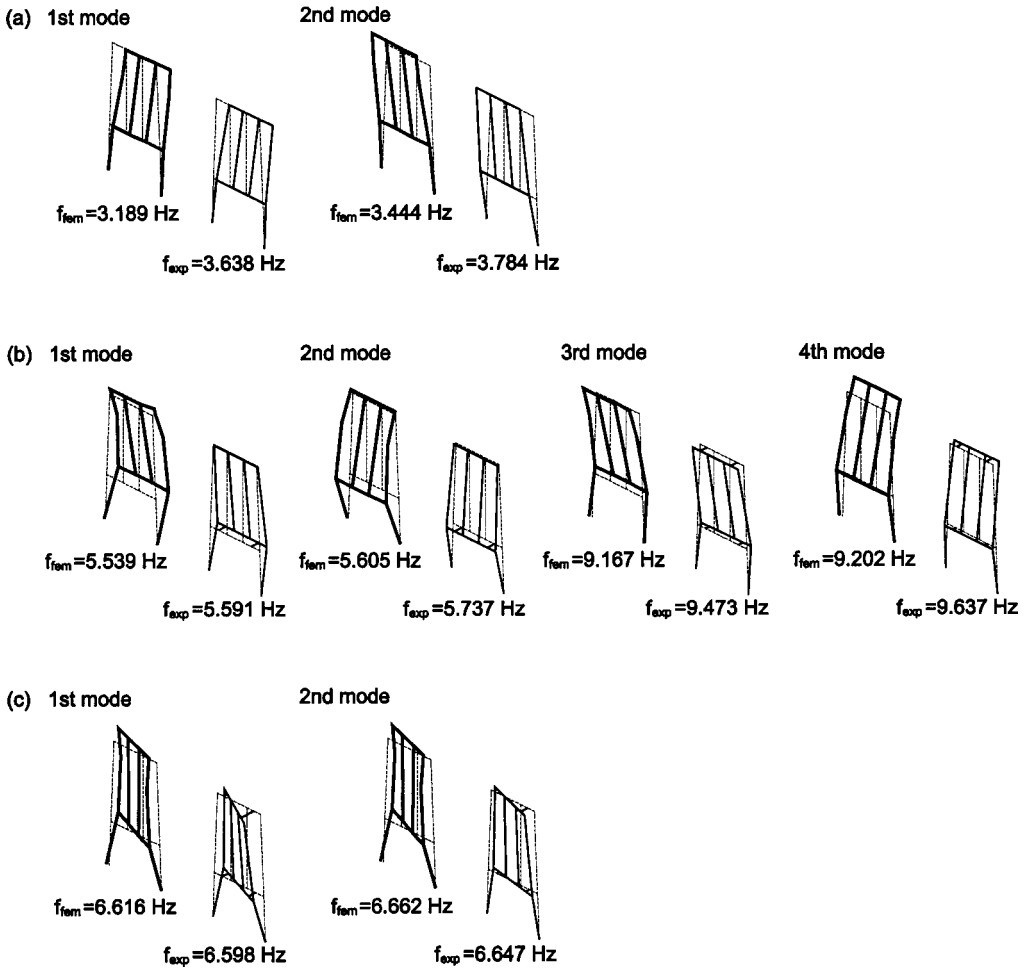

Table 3. Numerical and experimental frequencies of the deck.

Type	Numerical frequency (Hz)	Experimental frequency (Hz)	Type	Numerical frequency (Hz)	Experimental frequency (Hz)
Flexure	0.63	0.65	Torsion	1.27	1.22
Flexure	0.82	0.87	Torsion	2.10	2.02
Flexure	1.29	1.48	Torsion	2.91	3.02
Flexure	2.04	2.39	Torsion	4.16	4.42
Flexure	3.11	3.50	Torsion	5.33	5.51
Flexure	4.27	4.68	Torsion	6.68	6.77
Flexure	5.46	5.96	Torsion	7.77	8.48
Flexure	6.74	7.18	Torsion	9.58	9.76
Flexure	8.16	8.47			
Flexure	9.54	9.72			

To account for sagging effects, the modulus of elasticity of the stays was adjusted according to the following (Walter et al. 1985):

$$[1] \qquad E_{\text{eq}} = \frac{E_{\text{s}}}{1 + [(\gamma \ell)^2/(12\sigma^3)]E_{\text{s}}}$$

where σ is the tensile stress in cable, E_{s} is the cable modulus of elasticity, and γ is the cable volumetric weight. The horizontal projection of the stay is given by $\ell = s\cos\alpha$, with s being the chord length and α chord inclination.

The stiffening girders and transverse bracing system were modeled with 3D truss elements and the towers were modeled with 3D beam elements. The orthotropic deck was modeled with plate elements having membrane and flexural stiffness.

Fig. 12. Determination of the dynamic amplification factor, single truck (right lane) at 76 km/h: (*a*) recorded and computed static displacements and (*b*) corresponding truck passage.

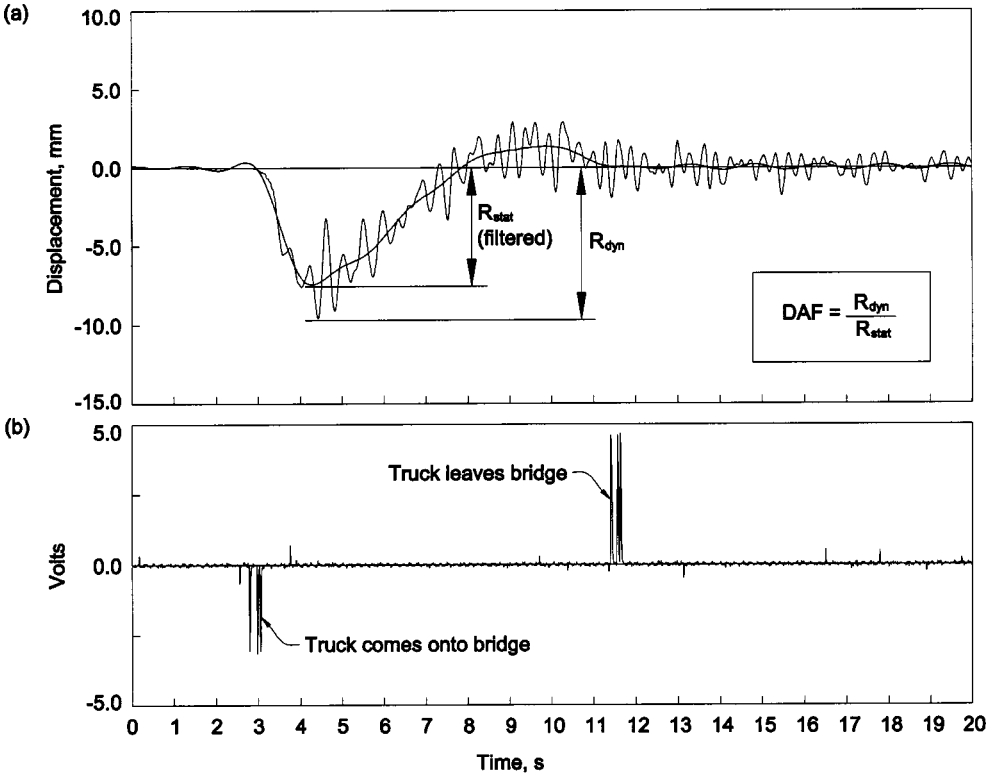

Table 4. MAC values for the first four flexural and four torsional modes.

Mode	1	2	3	4	5	6	7	8
1	**0.9385**	0.0016	0.0110	0.0071	0.0000	0.0000	0.0008	0.0000
2	0.0016	**0.9527**	0.0000	0.0001	0.0056	0.0002	0.0001	0.0000
3	0.0013	0.0000	**0.9350**	0.0111	0.0000	0.0000	0.0471	0.0001
4	0.0157	0.0000	0.0062	**0.9289**	0.0000	0.0000	0.0097	0.0000
5	0.0000	0.0002	0.0002	0.0000	**0.9069**	0.0604	0.0098	0.0026
6	0.0000	0.0171	0.0000	0.0000	0.0279	**0.8179**	0.0001	0.0098
7	0.0000	0.0000	0.0025	0.0008	0.0002	0.0000	**0.9167**	0.0011
8	0.0000	0.0000	0.0000	0.0000	0.0877	0.0121	0.0071	**0.7773**

All stiffening ribs in the longitudinal direction of the steel deck were modeled with 3D beam elements (not shown in Fig. 9).

The numerical correlation studies showed that secondary elements (sidewalk, parapet, etc.) did not play significant roles in the stiffness of the bridge. Consequently, their added masses were considered in the model. Separate plate elements with no stiffness were used to account for the uniform mass of the pavement. The original thickness of the pavement was reduced as a result of normal wear and tear; the thickness values measured at test time were used.

The dynamic properties of the bridge were calculated by subspace iteration after initialization of cable tension by an iterative procedure. A total of 89 modes were obtained in the 0–10 Hz range. This includes 23 deck modes and 8 tower modes as well as 58 cable and local modes. Table 3 lists the 18 vertical flexural and torsional frequencies obtained for the deck (four lateral flexural modes and one longitudinal mode were also obtained). These are compared with experimental findings. Figure 10 shows the first six flexural and torsional modes identified from ambient data. For each mode, these shapes are compared with predicted finite element modes. The excellent agreement between measured and computed dynamic properties is confirmed by the modal assurance criterion (MAC) given by

$$[2] \qquad \mathrm{MAC}_{i,j} = \frac{|\phi_{\mathrm{e},i}^{\mathrm{T}} \phi_{\mathrm{n},j}|^2}{\phi_{\mathrm{e},i}^{\mathrm{T}} \phi_{\mathrm{e},i} \phi_{\mathrm{n},j}^{\mathrm{T}} \phi_{\mathrm{n},j}}$$

where $\phi_{\mathrm{e},i}$ is the experimental shape for mode i and $\phi_{\mathrm{n},j}$ is the numerical shape for mode j(Allemang and Brown, 1982). Table 4 shows MAC values for the first four flexural and torsional modes. Good correlation between experimental and analytical

Fig. 13. Integration of acceleration responses, single truck (right lane) at 76 km/h: (*a*) effect of baseline correction and (*b*) comparison of integrated acceleration and measured displacement.

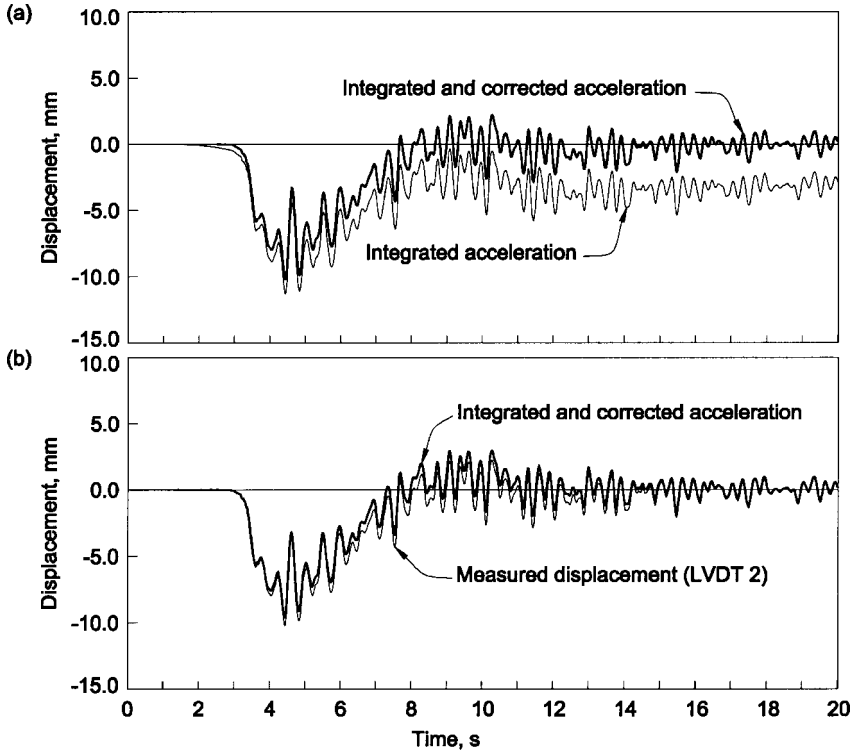

data for a given mode will result in a diagonal value ($MAC_{k,k}$) close to one and off-diagonal terms close to zero. Similar agreement was obtained for all deck and tower modes (Bégin, 1995).

7. Dynamic amplification factor

The evaluation of the dynamic amplification factor was the main objective of the Beauharnois Bridge tests. Typically, displacement and strain values are used to obtain the DAF. However, due to the strong current of the Saint Lawrence River, it was impossible to set up displacement transducers underneath the main girder. Only two locations were therefore instrumented with LVDTs positioned close to the east tower (Fig. 3*b*). Consequently, displacement time histories were obtained by integrating acceleration recordings for each measurement station and used to compute displacement DAFs.

The DAF is defined as the ratio of the maximum dynamic response to the maximum static response. This definition has been widely used by researchers to compute the DAF from experimental data. However, the values used for maximum static and dynamic responses have been subjected to interpretation (Paultre et al. 1992). In this project, the maximum dynamic responses were obtained from displacements, integrated acceleration recordings, and strain recordings. The maximum static responses were computed by applying a lowpass digital filter to remove the dynamic components from these recordings. The resulting "static" responses, not necessarily occurring at the same time as the maximum dynamic response, were also compared with recordings obtained during quasi-static low-speed tests (below 15 km/h).

Figure 12 shows the recorded displacement on LVDT 2 (see Fig. 3*b*), obtained during a test run completed with a single truck at a speed of 76 km/h. The "static" response, computed with a moving weighted-average time-domain digital filter, is superimposed on the dynamic recording. The maximum dynamic response, R_{dyn}, and the maximum filtered static response, R_{stat}, are also indicated. The displacement DAF is taken as the ratio of these two values. Different DAF values obtained with this technique are averaged with respect to vehicle speed, loading patterns, and position on the bridge.

Although displacement and strain measurements are usually preferred for evaluating the DAF, acceleration data can be integrated to obtain a reliable estimate of the displacement and, therefore, of the DAF. During the integration process, a constant shift in acceleration translates into a linear shift for speed and a parabolic shift in displacement that will corrupt the final result. A baseline correction is therefore applied to the data. The remaining offsets due to the presence of very low frequency components in the integrated displacements are eliminated by a high-pass digital filter.

The two curves in Fig. 13*a* show the displacements obtained by (*i*) integrating the acceleration with a baseline correction and (*ii*) correcting the resulting displacement with a high pass filter. The filter cutoff frequency is selected below the frequency corresponding to the half-sine of the "static" displacement. The integration and filtering process is calibrated by comparing measured displacements from an LVDT and integrated displacements from an accelerometer positioned next to the LVDT. Figure 13*b* shows that the integration process, with appropriate corrections, results in a displacement signal that agrees with data directly obtained with an LVDT.

Table 5. Average DAF values.

	Strain[a]		Strain[b]		Displacement[c]		Acceleration[d]	
Vehicle(s)	min.	max.	min.	max.	min.	max.	min.	max.
Single truck	1.28	1.29	1.19	1.20	1.10	1.11	1.06	1.07
Truck and trailer	1.12	1.13	1.08	1.09	1.03	1.04	1.01	1.02
2 trucks side-by-side	1.19	1.20	1.09	1.10	1.05	1.06	1.03	1.03
2 trucks in line	1.24	1.24	1.10	1.10	1.06	1.07	1.04	1.05
Average, all tests	1.20	1.21	1.12	1.12	1.07	1.07	1.03	1.04

[a] Strain DAF from strain gauges on hangers.
[b] Strain DAF from strain gauges on the main girder.
[c] Displacement DAF from LVDTs.
[d] Integrated acceleration DAF from accelerometers.

Table 5 shows the average values of the DAF for strain measurements obtained on the hangers and on the deck (see Fig. 3). Displacement DAF values computed from LVDT recordings and integrated acceleration signals are also shown. The DAFs are given for different load cases; the mimimum and maximum values correspond to the upper and lower limits of the filter parameters used to extract the static response. It is interesting to note that, for all types of measurement, the dynamic amplification is higher in the case of single-truck loading.

The table also shows that DAF values for strain are higher than those computed for displacement or integrated acceleration. This difference in dynamic amplification can be explained by the following observations. It can be shown by modal superposition that the elastic force response, which is proportional to strain response, is also proportional to the frequency squared, whereas displacements are not. If higher modes are excited by bridge–vehicle interaction, larger responses can be expected for force (and strain) responses than for displacement responses.

8. Conclusions

The reliable and inexpensive procedures for dynamic testing described in this paper were applied to a rehabilitated hybrid suspension and cable-stayed bridge. The dynamic properties were obtained for the bridge under ambient traffic loading. Modal analysis techniques were used and a total of 31 deck and tower modes were identified. These results were used in a numerical correlation study carried with a 3D finite element model that accounted for nonlinear cable behaviour. Excellent agreement was observed between experimental and numerical mode shapes. An important objective of the tests was the evaluation of the dynamic amplification factor, as this is rarely measured for suspension and cable-stayed bridges. The DAF was computed for displacements, strains, and integrated acceleration responses. It was shown that the integration of acceleration data with baseline correction and filtering yielded reliable estimates of the displacement DAFs. Such experimental results are inexpensive and extremely useful for numerical model calibration. They also complete the existing database for dynamic amplification factors used in design codes. There is, however, a need for more experimental data obtained on long, flexible suspension bridges. It is hoped that the results presented here will contribute toward the development of a database for suspension bridges.

Acknowledgements

The authors gratefully acknowledge the support of the Quebec Ministry of Transportation and Hydro-Québec for their contribution to this project. The authors are also grateful to the Natural Sciences and Engineering Research Council of Canada for its continuing support.

References

Allemang, R.J., and Brown, D.L. 1982. A correlation coefficient for modal vector analysis. Proceedings of the 1st International Modal Analysis Conference, Orlando, Fla., pp. 110–116.

Bégin, T. 1995. Experimental and analytical study of the dynamic behaviour of Beauharnois suspension bridge. (In French.) M.Sc. thesis, Département de génie civil, Université de Sherbrooke, Sherbrooke, Que.

Muria-Vila, D., Gomez, R., and King. C. 1991. Dynamic structural properties of cable-stayed Tampico Bridge. ASCE Journal of Structural Engineering, **117**(11): 3396–3416.

Paultre, P., Chaallal, O., and Proulx, J. 1992. Bridge dynamics and dynamic amplification factors — a review of analytical and experimental findings. Canadian Journal of Civil Engineering, **19**(2): 260–278.

Paultre, P., Proulx, J., and Talbot, M. 1995. Dynamic testing procedures for highway bridges using traffic loads. ASCE Journal of Structural Engineering, **121**(2): 362–376.

Stiemer, S.F., Taylor, P., and Vincent, D.H.C. 1988. Full scale dynamic testing of the Annacis Bridge. IABSE Proceedings P-122/88.

Walter, R., Houriet, B., Isler, W., and Moia, P. 1985. Cable-stayed bridges. (In French.) Presses polytechniques romandes, Lausanne, Switzerland.

Wilson, J.C., and Liu, T. 1991. Ambient vibration measurements on a cable-stayed bridge. Earthquake Engineering and Structural Dynamics, **20**: 723–747.

Wilson, J.C., and Gravelle, W. 1991. Modelling of a cable-stayed bridge for dynamic analysis. Earthquake Engineering and Structural Dynamics, **20**: 707–721.